EUROPHYSICS LETTERS 1 June 2006

Europhys. Lett., **74** (5), pp. 916–922 (2006)
DOI: 10.1209/epl/i2005-10585-0

Osmotically induced passage of vesicles through narrow pores

G. T. Linke, R. Lipowsky and T. Gruhn

Max Planck Institute of Colloids and Interfaces - Science Park Golm D-14424 Potsdam, Germany

received 16 August 2005; accepted in final form 4 April 2006
published online 3 May 2006

PACS. 87.16.Dg – Membranes, bilayers, and vesicles.
PACS. 68.15.+e – Liquid thin films.
PACS. 87.16.Ac – Theory and modeling; computer simulation.

Abstract. – The osmotically induced passage of fluid vesicles through narrow pores is studied theoretically using Monte Carlo simulations and a recently introduced sampling scheme. The free energy barrier for this transport process is calculated explicitly. An essential part of the free energy barrier is based on thermal fluctuations of the membrane shape. Simulation results indicate that, in real systems, the passage can be driven by osmotic pressure alone. The dynamics of the passage process are dominated by the geometry-induced changes of the vesicle volume and the associated water permeation through the vesicle membrane. The passage time is estimated to be of the order of minutes.

In the last decades pharmacological research was not only directed towards new drugs but also towards new ways of drug delivery. Particularly important innovations have been made for the transdermal application [1] which is preferable to the oral route in many cases [2]. The human skin represents a large barrier for most molecules. Only for very small lipophilic molecules, a certain skin permeability is predicted [3]. Larger molecules and aggregates may only pass through hydrophilic pores in the stratum corneum, the outermost layer of the epidermis [4]. These pores have diameters of about 20–30 nm so that many colloids are still too large and stiff to be squeezed through [4]. Lipid vesicles, on the other hand, have a number of properties that make them attractive for transdermal transport [4]. It is claimed by some researchers that ultraflexible lipid vesicles can be sufficiently pushed to pass through pores [4,5]. In a numerical study, the penetration of vesicles into large pores was induced by a constant external force and was found to be strongly enhanced if this force exceeds a certain threshold value [6]. In a more recent letter, the effect of a strongly attractive pore wall on the passage process has been investigated [7].

Across the skin there is a steep gradient in humidity, such that there is a lower salt concentration in the deeper skin layers. Therefore an osmotic pressure pushes the vesicle through the pore [5]. It is not yet clear how deep intact liposomes actually move into the skin [5,8]. Nevertheless, if liposomes filled with drugs are able to pass through skin pores, the drugs spread out under the skin as the vesicle finally ruptures.

In contrast to previous studies [6,7], we consider the osmotic force as the main driving force for the transport of a lipid vesicle through a narrow skin pore. Using extensive Monte Carlo simulations and a recently developed sampling scheme [9] we obtained the free energy barrier

© EDP Sciences
Article published by EDP Sciences and available at http://www.edpsciences.org/epl or http://dx.doi.org/10.1209/epl/i2005-10585-0

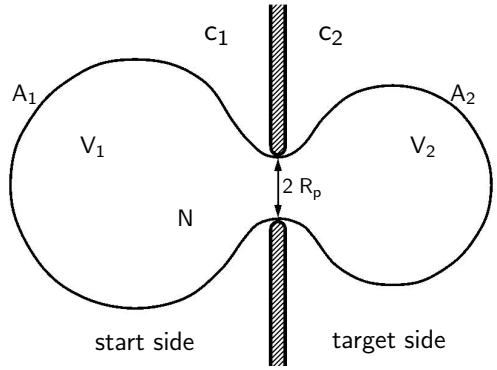

Fig. 1 – Vesicle in a narrow pore of radius R_p. The concentrations of osmotically active particles on both sides of the pore are c_1 and c_2, respectively, N is the number of osmotically active particles inside the vesicle. A_1 and A_2 are the membrane parts, V_1 and V_2 are the volume parts on the start and the target side, respectively.

for the transport process through the pore. A successful vesicle passage is indicated by the vanishing of the free energy barrier, which occurs for sufficiently large concentration gradients. As a consequence, it becomes evident for the first time that vesicle transport through skin pores can be driven by osmotic pressure alone.

The model system. – We consider a vesicle with a fixed membrane area $A = 4\pi R_0^2$ and a variable volume V in front of a pore in a skin layer, mimicked by a circular hole with radius R_p in a thin impenetrable wall (see fig. 1). During the passage, a part V_1 of the vesicle volume is on one side and a part V_2 is on the other side of the wall, such that $V = V_1 + V_2$. Analogously, we divide the constant surface area A into $A = A_1 + A_2$. The pore radius is always chosen to be $R_p = 0.35\, R_0$. For simplicity, the pore length is set to zero.

We assume that the passage through the pore is mainly governed by the osmotic conditions, the pore geometry, the bending elasticity of the vesicle membrane, and the membrane's permeability to water. In the absence of a spontaneous curvature the bending energy of the vesicle membrane with bending rigidity κ can be expressed as [10]

$$E_{el} = 2\kappa \oint M^2 \, \mathrm{d}A, \tag{1}$$

where M is the local mean curvature. An osmotic pressure acts on both parts of the vesicle, affected by osmotically active molecules which cannot permeate through the vesicle membrane. Across the pore we assume a concentration gradient of osmotically active molecules with a concentration c_1 on the side where the vesicle starts and a concentration $c_2 < c_1$ on the target side. As for the homogeneous case [11], integration of van't Hoff's law [12] provides an osmotic energy expression. With a reference volume V_{ref} and a number of N osmotically active molecules inside the vesicle one obtains

$$E_{osm} = T\left(-N \ln \frac{V}{V_{ref}} + c_1 V_1 + c_2 V_2\right), \tag{2}$$

where T is the thermal energy, including the Boltzmann constant. It follows from eq. (2) that the osmotic energy difference between a vesicle with volume V on the start and the target side is given by $\Delta E_{osm} = -TV(c_1 - c_2) < 0$ which is the basic driving force for the transduction.

The simulations were performed with $\kappa = 5$–$20\,T$. The hydrodynamic effects arising from the surrounding water and adhesion effects between membrane and skin cells were assumed to be small. In *in vitro* experiments with vesicles, the concentrations c of osmotically active particles are typically of the order of $c = 10^{-4}\,\mathrm{mol\,m^{-3}}$, *i. e.* $cVT \simeq 10^3\kappa$. Accordingly, we chose $c_2 = 2650/R_0^3$ on the target side and $N = 10000$, so that $N/V \simeq c_2$ if the vesicle is almost spherical. The concentration c_1 on the start side was varied to study its influence on the passage process.

Simulation methods. – In our Monte Carlo simulations the fluid vesicle is represented by a closed dynamically triangulated surface [13] with 596 triangles and edge lengths according to the original tethered-beads model [14]. The total area is kept fixed, up to a small interval. For the discretization of the bending energy a scheme proposed in [15] is used. Five types of Monte Carlo moves are applied in random order: Independent moves of single vertices (I) make 12%, bond-flips [13] (II) in which an edge between two triangles is relocated to connect the formerly unconnected vertices of the two triangles make 18%, reflections of a vertex by the osculating plane defined by the vertex' nearest neighbors (III) make 10%, moves of single vertices parallel to the wall for vertices which are close to the pore wall (IV) make 25% and bond-flips in the same region (V) make the remaining 35% of all moves. As the coordinates of the nearest neighbors remain invariant during the move of a certain vertex, moves of type (III) obey detailed balance. For moves of type (IV) and (V), distances of vertices and edges from the wall remain constant, and detailed balance is again fulfilled.

Free energy barrier. – As the vesicle passes the pore, a free energy barrier arises from an increase of the elastic energy, an increase of E_{osm} due to the reduction of the vesicle volume, and an entropy decrease since the confinement restricts the configuration space. During the passage the volume inside the vesicle changes significantly, while the intrinsic surface area of the vesicle is almost constant. The part A_2 of the surface area on the target side changes continuously and is, thus, suitable for the parametrization of the passage process. Consequently, energetic barriers to the passage will appear as barriers in the restricted free energy of the vesicle for a given A_2

$$F\left(A_2\right) \equiv -T \ln \int \mathrm{d}\Gamma\, e^{-\frac{E_{el}+E_{osm}}{T}}\, \delta\left(A_2'\left(\Gamma\right) - A_2\right). \tag{3}$$

The integration in eq. (3) takes place over all vesicle configurations that do not overlap with the pore wall. While the passage through the pore is a non-equilibrium process, fixing A_2 defines an equilibrium state. Thus, the free energy $F(A_2)$ can be obtained with Monte Carlo simulations and a recently proposed integration scheme [9] up to a constant F_0.

For relatively small osmolarities $c_1 = 2700/R_0^3$ on the start side, we observe a barrier in the restricted free energy $F(A_2)$, which is almost independent of the bending rigidity in the range of $3.5 \leq \kappa/T \leq 15$ (see fig. 2). As shown in fig. 3, $F(A_2)$ is more sensitive to the osmotic conditions. The free energy barrier decreases with increasing c_1. The critical osmolarity on the start side, where the free energy barrier disappears, is approximately $c_1 \approx 3000/R_0^3$.

Limit of spherical caps. – As shown in fig. 2, the influence of the elastic energy on $F(A_2)$ is small in the range $3.5 \leq \kappa/T \leq 15$. If the osmotic particle concentrations in- and outside the vesicle are large and the temperature T is low, the osmotic energy E_{osm} dominates the passage process. In the following we compare the behavior of $E_{osm}(A_2)$ with the full free energy $F(A_2)$ and derive an analytic criterion for a vanishing barrier of $E_{osm}(A_2)$ which is a minimum requirement for a successful vesicle passage at finite T. For $N/V > c_1 > c_2$, the derivatives $\mathrm{d}E_{osm}/\mathrm{d}V_i$ for $i = 1, 2$ are negative, so that the system favors maximum volumes

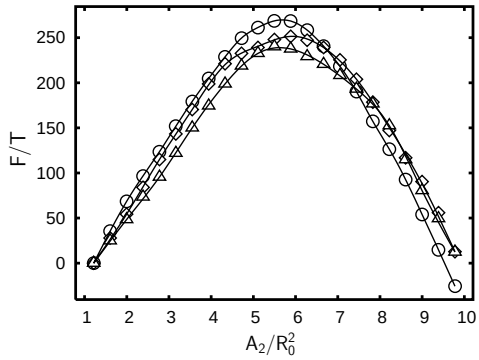

Fig. 2

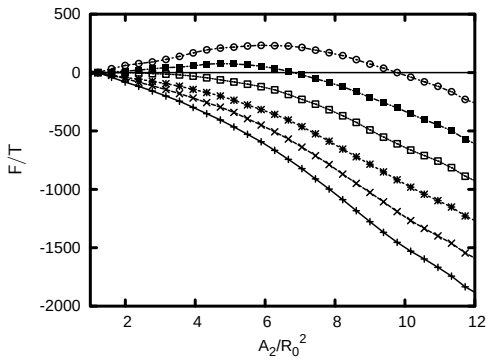

Fig. 3

Fig. 2 – Free energy F in units of the thermal energy T as function of the area A_2 for $c_1 = 2700/R_0^3$ and $\kappa = 3.5\,T$ ($\circ$), $\kappa = 9\,T$ ($\diamond$), $\kappa = 15\,T$ ($\triangle$).

Fig. 3 – Same as fig. 2 for $\kappa = 10\,T$ and $c_1 = 2700/R_0^3$ ($\circ$), $c_1 = 2800/R_0^3$ ($\blacksquare$), $c_1 = 2900/R_0^3$ ($\boxdot$), $c_1 = 3000/R_0^3$ ($*$), $c_1 = 3100/R_0^3$ ($\times$), $c_1 = 3200/R_0^3$ ($+$).

V_1 and V_2, which for given A_1 and A_2 are realized by spherical caps with

$$V_i = \frac{1}{6\sqrt{\pi}}\sqrt{A_i - \pi R_p^2}\,\left(A_i + 2\pi R_p^2\right) \qquad (i = 1, 2). \tag{4}$$

In the limit of spherical caps, eqs. (2) and (4) and $A_1 = A - A_2$, can be used to express the osmotic energy E_{osm} as a function of A_2. Plots of $E_{osm}(A_2)$ are shown in fig. 4 for various start side concentrations c_1. The curves are qualitatively similar to the free energies in fig. 3 but the barrier height of $E_{osm}(A_2)$ is distinctly lower than that of $F(A_2)$ and vanishes already for $c_1 \approx 2750/R_0^3$.

A spherical vesicle with the maximum volume $V_0 \equiv 4\pi/3\,R_0^3$ can partially enter the pore without any deformation. The target side area of an undeformed vesicle can be up to $A_{2,0} \equiv \frac{A}{2}(1 - \sqrt{1 - (R_p/R_0)})$. In the limit of spherical caps, a successful vesicle passage requires that for all $A_2 \equiv (1+q)A_{2,0}$ with $q \geq 0$ the driving force of the transport process $-\mathrm{d}E_{osm}(A_2)/\mathrm{d}A_2$ must be positive. In principle, the condition

$$\max_{q \geq 0} \left(\left. \frac{\mathrm{d}E_{osm}}{\mathrm{d}A_2} \right|_{A_2 = (1+q)A_{2,0}} \right) < 0 \tag{5}$$

can always be fulfilled by a suitably high start side concentration c_1. Linearizing the left-hand side of relation (5) with respect to R_p provides the simple condition

$$c_1 > c_2 + \left(1 - \frac{R_p}{R_0}\right)\left(\frac{N}{V_0} - c_2\right). \tag{6}$$

In fig. 5, the minimum concentrations c_1 according to relation (5) and relation (6), respectively, shows the good agreement of the two conditions.

In cases, where thermal fluctuations or the elastic energy are relevant, the volumes V_1 and V_2 are always smaller than the maximum values in eq. (4). The sensitivity of E_{osm} on such volume reductions is demonstrated by the fourth curve in fig. 4, which shows $E_{osm}(A_2)$ for $c_1 = 2700/R_0^3$ if the sharp kink between the spherical caps is replaced by a membrane cylinder of diameter $2R_p$ and length R_p. With this constraint the barrier height of $E_{osm}(A_2)$ increases

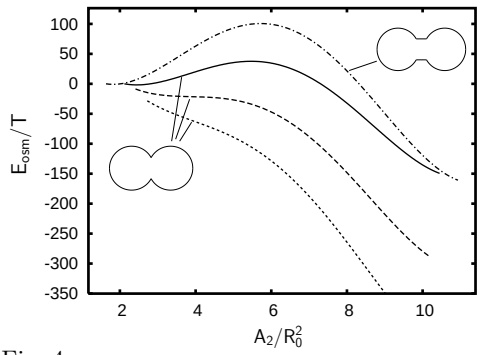

Fig. 4

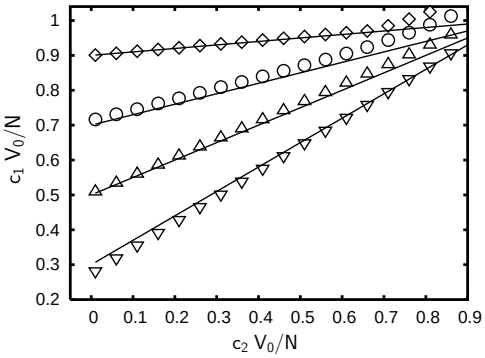

Fig. 5

Fig. 4 – Osmotic energy for a vesicle consisting of two spherical caps with a start side concentration $c_1 = 2700/R_0^3$ (—), $c_1 = 2750/R_0^3$ (−−), and $c_1 = 2800/R_0^3$ $(\cdots)$, as well as for a vesicle geometry with two spherical caps connected by a cylinder of length $l = R_p$ with $c_1 = 2700/R_0^3$ $(-\cdot-)$.

Fig. 5 – Minimum start side concentrations c_1 that provide a monotonously decaying osmotic energy $E_{osm}(A_2)$ for a given target side concentration c_2. Both, c_1 and c_2, are given in units of N/V_0, where N is the number of osmotically active molecules inside the vesicle and $V_0 \equiv \frac{4\pi}{3}R_0^3$ is the maximum vesicle volume. Results are shown for pore radii $R_p = 0.1R_0$ $(\diamond)$, $R_p = 0.3R_0$ $(\circ)$, $R_p = 0.5R_0$ $(\triangle)$, $R_p = 0.7R_0(\nabla)$, where lines represent the right-hand side of relation (6).

by more than a factor of 2, but is still distinctly smaller than the barrier height of $F(A_2)$ for the same c_1. This indicates that thermal fluctuations of the membrane shape cause a strong increase of the free energy barrier under the conditions used in our simulations.

Dynamics of pore passage. – In general, the passage process can be divided into four different elementary processes with different time scales: Changes of $V_1 - V_2$ are faster than the relaxation of A_2 which depends on the viscosity $\nu \simeq 10^{-7}\,\mathrm{N\,s\,m^{-1}}$ [16] and the intermonolayer friction coefficient $\eta_r \simeq 10^8\,\mathrm{N\,s\,m^{-3}}$ [17] of the membrane with a characteristic time scale of the order of milliseconds for vesicles with radii $R_0 = 10\,\mu$m. Fluctuation modes of such vesicles decay within some seconds [18] whereas osmotically induced changes of the vesicle volume occur within minutes and define the dominating time scale. The basic aspect of the osmotically driven transport of the membrane is the decrease of V_1 and the increase of V_2. Thus, the whole process is dominated by the permeation-dependent dynamics of $V(t)$. The change of $V(t)$ is governed by the evolution equation [19]

$$\dot{V} = -A\frac{C_{pe}}{T}\left.\frac{\partial \tilde{F}}{\partial V}\right|_{A_2(V)}. \tag{7}$$

Here, C_{pe} is the permeation constant of the membrane and

$$\tilde{F}(A_2, V) \equiv -T \ln \int \mathrm{d}\Gamma\, e^{-\frac{E_{el}+E_{osm}}{T}}\, \delta\left(A_2'(\Gamma) - A_2\right) \delta\left(V'(\Gamma) - V\right) \tag{8}$$

is the restricted free energy with respect to the area A_2 on the target side and the volume V, which has to be calculated in order to determine the right-hand side of eq. (7).

While the total volume V changes slowly, the values of $V_1 - V_2$ and A_2 fluctuate around their equilibrium values corresponding to $V(t)$. Hence, the membrane area A_2 on the target side stays always in the same local minimum of the restricted free energy for a given volume

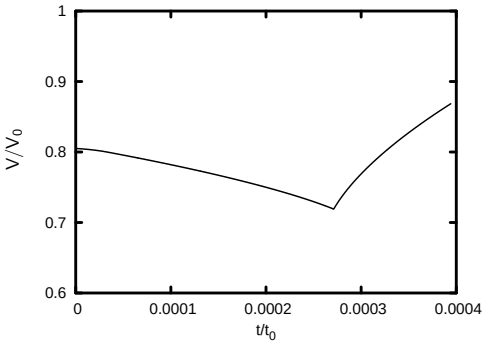

Fig. 6

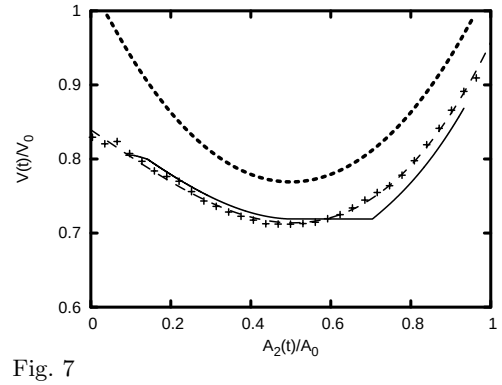

Fig. 7

Fig. 6 – Vesicle volume V as a function of time.

Fig. 7 – Time evolution of the vesicle volume $V(t)$ during the passage process as function of the surface area $A_2(t)$ on the target side (solid line) compared to the average vesicle volume. The dashed line is a fit to the simulation results ($+++$). The finite pore size defines a maximum volume (dotted line). The reference area A_0 is given by $A_0 \equiv 4\pi\, R_0^2$ and the reference volume by $V_0 \equiv 4\pi/3\, R_0^3$.

V. The free energy has an absolute minimum for $A_2 \lesssim 4\pi R_0^2$, corresponding to a vesicle which is almost entirely on the target side. For large enough V, there is also a local minimum of $\tilde{F}(A_2, V)$ for a small value of A_2, corresponding to a vesicle which has partially entered the pore. If the local minimum does not disappear, the vesicle gets stuck inside the pore. With these considerations, the dynamics of the membrane transport can be analyzed. The probability distribution of V for a given A_2 is obtained from Monte Carlo simulations and our new sampling scheme and reveals an almost Gaussian shape. Thus, the free energy can be approximated by

$$\tilde{F}(A_2, V) = F(A_2) + \frac{T}{2} \frac{(V - \langle V|A_2\rangle)^2}{\mathrm{Var}[V|A_2]}, \tag{9}$$

where $\langle V|A_2\rangle$ is the mean value and $\mathrm{Var}[V|A_2]$ is the variance of the vesicle volume for a given surface area A_2 on the target side. Neglecting hydrodynamic effects in the surrounding water, the change of the volume is given by

$$\dot{V} = -A \frac{C_{pe}}{T} \left.\frac{\partial \tilde{F}}{\partial V}\right|_{A_2(V)} = -4\pi R_0^2 C_{pe} \frac{V - \langle V|A_2(V)\rangle}{\mathrm{Var}[V|A_2(V)]}, \tag{10}$$

where $A_2(V(t))$ is the equilibrium value of the surface area on the target side as described above. Note that mean value and variance refer to thermal equilibrium while the current volume is a non-equilibrium quantity.

We have integrated eq. (10) with values for $\tilde{F}(A_2, V)$ from a simulation with $\kappa = 7\,T$, $c_1 = 3000/R_0^3$ and $c_2 = 2650/R_0^3$. The vesicle volume V is plotted in fig. 6 as a function of time in units of $t_0 \equiv R_0^4/C_{pe}$. Figure 7 shows the volume as a function of A_2 and $\langle V|A_2\rangle$ as calculated from the equilibrium simulations with given A_2. Finally, we estimate the time scale on which the passage process takes place. As the passage through the pore includes a reduction of the initial vesicle volume $V(0)$ to a value $\alpha V(0) < V(0)$ with an almost constant efflux $\dot{V}$, the passage time t_{pas} can be derived from

$$V(0) + t_{pas}\dot{V}(0) = \alpha V(0). \tag{11}$$

The dimensionless parameter α is the same for simulations and for real experiments. Thus, writing eq. (11) for both cases and eliminating α relates the ratio of the passage times for simulation and experiment to the ratio of according length scales, initial concentration differences, and permeation constants. If we set $t_0 = (R_0^4/C_{pe})_{sim}$, $\Delta c_{sim} = 350/R_0^3$, $t_{pas,sim} \simeq 2.7 \cdot 10^{-4}\, t_0$, $C_{pe,exp} = C_{pe,f}\nu_{H_2O}$ with $C_{pe,f} \simeq 100\,\mu\mathrm{m\,s^{-1}}$ [19,20] and $\nu_{H_2O} = 18\,\mathrm{ml/mol}$, $R_{0,exp} = 10\,\mu\mathrm{m}$, and $\Delta c_{exp} = 1\,\mathrm{mmol/l}$, we get

$$t_{pas,exp} = \frac{(C_{pe}/R_0\,\Delta c)_{sim}}{(C_{pe}/R_0\,\Delta c)_{exp}} t_{pas,sim} \approx 9\,\mathrm{min}. \tag{12}$$

As the passage time $t_{pas,exp}$ is of the order of minutes, the osmotically driven vesicle transport through narrow pores is fast enough for scientific and practical applications.

Discussion. – The influence of osmotic pressures on the passage of fluid vesicles through narrow pores has been investigated. The free energy barrier for the passage process is strongly increased by thermal fluctuations of the membrane shape. Using Monte Carlo simulations, we have shown that a realistic concentration gradient of osmotically active molecules is sufficient to overcome the free energy barrier.

REFERENCES

[1] Mezei M. M. and Gulasekharam V., *Life Sci.*, **26** (1980) 1473.
[2] Prausnitz M. R., Mitragotri S. and Langer R., *Nat. Rev. Drug Discov.*, **3** (2004) 115.
[3] Potts R. O. and Guy R. H., *Pharm. Res.*, **9** (1992) 663; **12** (1995) 1628.
[4] Cevc G., *Crit. Rev. Drug Carrier Syst.*, **13** (1996) 257; *Adv. Drug Deliv. Rev.*, **56** (2004) 675.
[5] Cevc G. and Blume G., *Biochim. Biophys. Acta*, **1104** (1992) 226.
[6] Gompper G. and Kroll D. M., *Phys. Rev. E*, **52** (1995) 4198.
[7] Tordeux C. and Fournier J.-B., *Europhys. Lett.*, **60** (2002) 875.
[8] Lasch J., Laub R. and Wohlrab W., *J. Control. Release*, **18** (1991) 55; du Plessis J., Ramachandran C., Weiner N. and Müller D. G., *Int. J. Pharm.*, **103** (1994) 277; Betz G., Nowbakht P., Imboden R. and Imanidis G., *Int. J. Pharm.*, **228** (2001) 147; Verma D. D., Verma S., Blume G. and Fahr A., *Int. J. Pharm.*, **258** (2003) 141.
[9] Linke G. T., Lipowsky R. and Gruhn T., *Phys. Rev. E*, **71** (2005) 051602.
[10] Canham P. B., *J. Theor. Biol.*, **26** (1970) 61; Helfrich W., *Z. Naturforsch.*, **28c** (1973) 693.
[11] Seifert U., Berndl K. and Lipowsky R., *Phys. Rev. E*, **44** (1991) 1182.
[12] Reichl L. E., *A Modern Course in Statistical Physics* (Wiley, New York) 1998.
[13] Ho H.-S. and Baumgärtner A., *Europhys. Lett.*, **12** (1990) 295; *Phys. Rev. A*, **41** (1990) 5747; Kroll D. M. and Gompper G., *Science*, **255** (1992) 968; Gompper G. and Kroll D. M., in *Statistical Mechanics of Membranes and Surfaces*, edited by Nelson D., Piran T. and Weinberg S. (World Scientific, Singapore) 2004, pp. 359-426.
[14] Kantor Y., Kardar M. and Nelson D. R., *Phys. Rev. Lett.*, **57** (1986) 791.
[15] Jülicher F., Seifert U. and Lipowsky R., *Phys. Rev. Lett.*, **71** (1993) 452.
[16] Waugh R. E., *Biophys. J.*, **38** (1982) 19; 29.
[17] Evans E. and Yeung A., *Chem. Phys. Lipids*, **73** (1994) 39.
[18] Duwe H.-P., Käs J. and Sackmann E., *J. Phys. (Paris)*, **51** (1990) 945.
[19] Finkelstein A., *Water Movement Through Lipid Bilayers, Pores, and Plasma Membranes* (Wiley, New York) 1987.
[20] Fettiplace R. and Haydon D. A., *Physiol. Rev.*, **60** (1980) 510; Ye R. and Verkman A. S., *Biochemistry*, **28** (1989) 824; Olbrich K., Rawicz W., Needham D. and Evans E., *Biophys. J.*, **79** (2000) 321.